Comments and Addenda

The section Comments and Addenda is for short communications which are not appropriate for regular articles. It includes only the following types of communications: (1) Comments on papers previously published in **The Physical Review** *or* **Physical Review Letters.** *(2) Addenda to papers previously published in* **The Physical Review** *or* **Physical Review Letters,** *in which the additional information can be presented without the need for writing a complete article. Manuscripts intended for this section must be accompanied by a brief abstract for information-retrieval purposes. Accepted manuscripts follow the same publication schedule as articles in this journal, and page proofs are sent to authors.*

Spin-orbit coupling and electron scattering in concentrated *Au*Fe and *Au*Mn alloys

S. P. McAlister and C. M. Hurd
National Research Council of Canada, Ottawa, Canada K1A OR9
(Received 9 March 1979)

Concentrated *Au*Mn alloys show no side-jump contribution to their extraordinary Hall effect as the ferromagnetic percolation limit is approached. Comparable *Au*Fe alloys do. The difference is interpreted as evidence that side jump arises from electrons moving in clusters of ferromagnetically aligned groups of moments, and that the ferromagnetic environment is crucial. Practical difficulties in the extraction of the spin-orbit components of the Hall effect are discussed.

I. INTRODUCTION

Spin-orbit coupling of electrons during their scattering by localized magnetic moments can be revealed in two ways: as an asymmetric scattering cross section or as an effective displacement of the electron's wave packet. These are called skew scattering[1,2] and side-jump[3] effects, respectively. The former needs a scattering state with nonzero angular momentum while the latter is linked to band properties of electrons in a ferromagnetic environment. Either manifestation of spin-orbit coupling can add an extra component to the normal Hall field from the Lorentz force, giving an extraordinary Hall effect (EHE). Skew scattering is the dominant source of EHE in dilute alloys at low temperatures while the side-jump effect pertains to ferromagnets. Since the side-jump effect increases as the mean free path is reduced, it has been studied mostly in ferromagnets at relatively high temperatures.

We showed previously[4] that skew and side-jump effects are seen in the EHE of disordered *Au*Fe alloys at low temperatures. There is some question whether the side-jump effect requires a ferromagnetic environment because its contribution appears well below the ferromagnetic percolation limit. However, the effect is apparently associated with clusters of ferromagnetically aligned Fe moments formed as the percolation limit is approached.[5,6] Here we describe comparable measurements upon *Au*Mn alloys to test whether the ferromagnetic environment is essential for the side-jump effect. We also consider different ways the spin-orbit contribution to the EHE can be extracted—details which for lack of space could not be discussed previously.[4]

II. EXPERIMENTAL DETAILS AND RESULTS

We have measured at various temperatures in the range ~4–250 K the dependence on magnetic flux B of the Hall resistivity $\rho_{21}(B)$ and the total resistance $\rho_{11}(B)=\rho_{22}(B)$ of the alloys of Table I. Flux densities ranged to 7 T but low-field conditions ($\omega\tau \ll 1$, in the usual notation) were maintained throughout. (A free-electron metal having the resistivity of the most dilute sample of Table I has $\omega\tau < 10^{-2}$ at 4.2 K in 7 T.) The details of instrumentation and sample preparation are identical to those given previously.[7] Each sample was annealed at 1173 K in vacuum for 24 h before quenching into iced brine, and was stored at 77 K until measured.[8] The impurity resistivities ($\Delta\rho_0$ of Table I) agree quantitatively with previous results.[10,11]

For a given temperature, we obtain the field dependence of the Hall conductivity $\sigma_{21}(B)$ and magnetoresistance $\Delta\rho/\rho_{B=0}$ from the measured quantities using the usual formulas.[12] Figure 1 shows results for $\sigma_{21}(B)$ and $\rho_{21}(B)$ for the typical example of Au + 14 at.% Fe at 5 K. $\rho_{11}(B)$ is generally two orders of magnitude greater than $\rho_{21}(B)$, and the magnetoresistance is larger (Table I), so the variation of

TABLE I. Measured and calculated quantities at ~5 K. $\Delta\sigma_{21}$ and $\Delta\rho_{21}$ are the spin-orbit parts of the Hall conductivity and resistivity, $\Delta\rho_0$ is the impurity resistivity and $\Delta\rho(B)/\rho_{B=0}$ is the transverse magnetoresistance.

Concentration (at.%)	$\Delta\sigma_{21}$ ($10^3\ \Omega^{-1}\ m^{-1}$)	$\Delta\rho_0$ ($10^{-8}\ \Omega$ m)	$-\Delta\rho_{21}$ ($10^{-10}\ \Omega$ m)	$-\Delta\rho_{21}/(\Delta\rho_0)^2$ ($10^3\ \Omega^{-1}\ m^{-1}$)	$-\Delta\rho(B)/\rho_{B=0}$ (at 7 T)
		*Au*Fe			
1.1	48 ± 25	8.6	3.0 ± 2	40.5	0.091
2.6	4 ± 2	18.8	2.4 ± 1.5	6.79	0.069
5.0	1.6 ± 0.05	33.4	4.5 ± 0.9	4.03	0.074
8.2	2.6 ± 0.05	47.5	8.0 ± 0.5	3.55	0.147
11.0	2.9 ± 0.05	54.4	12.2 ± 0.1	4.12	0.220
13.0	3.6 ± 0.05	53.5	13.0 ± 0.05	4.54	0.262
14.0	4.9 ± 0.05	47.6	12.7 ± 0.05	5.60	0.272
14.8	5.7 ± 0.05	44.0	12.3 ± 0.05	6.35	0.277
16.8	7.1 ± 0.05	32.5	8.0 ± 0.05	7.50	0.254
		*Au*Mn			(at 6 T)
4.8	14.2 ± 0.05	9.16	4.0 ± 1.5	47.7	0.243
7.6	12.1 ± 0.05	18.9	7.5 ± 1.0	21.0	0.253
11.6	17.3 ± 0.05	22.5	10.0 ± 0.5	19.7	0.273
13.9	16.5 ± 0.05	26.2	12.3 ± 0.2	17.5	0.261
17.3	15.6 ± 0.05	29.6	15.0 ± 0.05	17.1	0.248

$\rho_{11}^2(B)$ in the denominator of $\sigma_{21}(B)$ cannot be neglected. As B increases, the spin-orbit contribution to the total Hall effect follows the magnetization to saturation, while for $\omega\tau << 1$ in a free-electron metal the Lorentz part varies linearly. The saturated spin-orbit part can thus in principle be obtained by extrapolating to $B=0$ the curves of Fig. 1, as illustrated. Frequently, the directly measured quantity $\rho_{21}(B)$ is

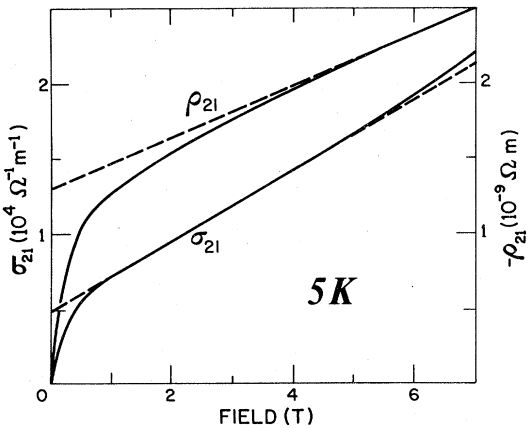

FIG. 1. Showing typical results, here for Au + 14-at.%-Fe. $\sigma_{21}(B)$ is calculated from the measured quantities $\rho_{21}(B)$ and $\rho_{11}(B)$. The extrapolations to zero field of $\rho_{21}(B)$ and $\sigma_{21}(B)$ give $\Delta\rho_{21}$ and $\Delta\sigma_{21}$, respectively.

used by writing it as the sum of two parts[2,13]

$$\rho_{21}(B)=\rho_{21}^{s.o.}(B)+\rho_{21}^{L}(B)\ ,$$

where the right-hand side comprises the spin-orbit and Lorentz parts, respectively. The latter is a "background" behavior varying linearly with field, so the saturated spin-orbit contribution is taken to be $\Delta\rho_{21}$, which is the ordinate obtained by extrapolating the saturated behavior of $\rho_{21}(B)$ to $B=0$. Strictly, this is incorrect because although the elements of the total magnetoconductivity tensor have additive components, those of the magnetoresistivity tensor do not. We therefore discuss[4] the saturated spin-orbit contribution to the total Hall conductivity $\Delta\sigma_{21}$, which is the corresponding quantity obtained by extrapolating $\sigma_{21}(B)$ to $B=0$.

Lack of saturation of $\rho_{21}(B)$ or $\sigma_{21}(B)$ in the range of fields available is a problem for the alloys below ~11 at.%, and sets a limit on the accuracy of $\Delta\sigma_{21}$. In the example of Fig. 1, the saturation of $\rho_{21}(B)$ is barely established at 7 T and would be worse in the more dilute samples. The linear section of $\sigma_{21}(B)$ used for extrapolation is also not without risk for this apparent saturation is partially an artifact arising from the inversion

$$\sigma_{21}(B)=-\rho_{21}(B)/[\rho_{11}^2(B)+\rho_{21}^2(B)]\ .$$

As B increases, ρ_{11}^2 decreases and exerts an increasing

influence in the denominator, eventually giving the upturn in $\sigma_{21}(B)$ seen above 5 T in Fig. 1; the opposite tendencies of $\rho_{21}^2(B)$ and $\rho_{11}^2(B)$ thus contribute to the apparent saturation of $\sigma_{21}(B)$ and it does not necessarily reflect the magnetization.

The spin-orbit part of the Hall conductivity for a given field is

$$\Delta\sigma_{21}(B) = \sigma_{21}(B) - \sigma_{21}^L(B) .$$

Since $\rho_{11} >> \rho_{21}$, this can be written approximately as

$$[\rho_{21}(B) - \rho_{21}^L(B)]/\rho_{11}^2(B) ,$$

so that for B extrapolated to zero $\Delta\sigma_{21} = \Delta\rho_{21}/(\Delta\rho_0)^2$,

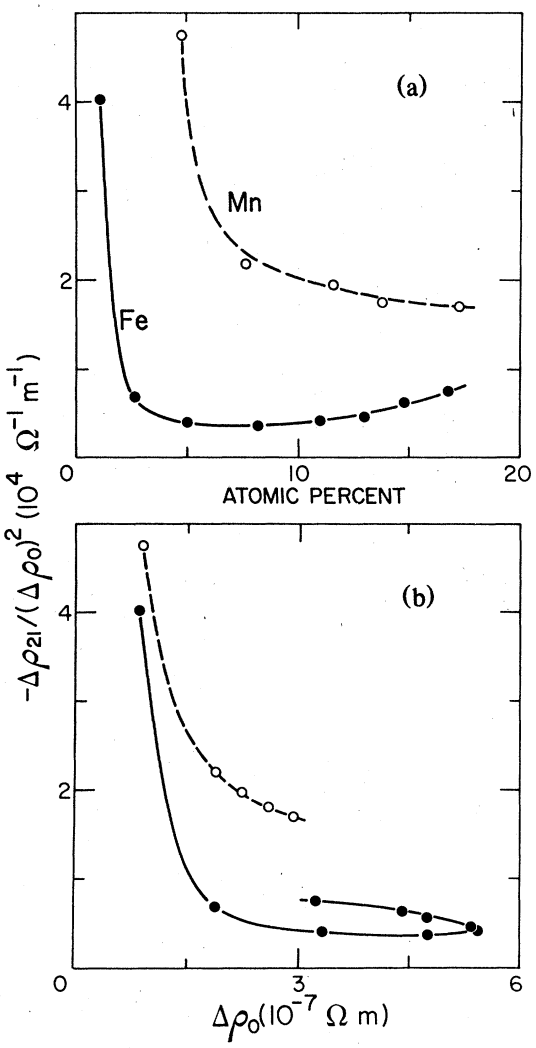

FIG. 2. Plot of the data from Table I showing $-\Delta\rho_{21}/(\Delta\rho_0)^2$, which is the lower limit of the spin-orbit contribution to the Hall conductivity ($\Delta\sigma_{21}$, defined in Fig. 1), against solute concentration or impurity resistivity ($\Delta\rho_0$). The results apply to ~5 K. In Figs. 2 and 3 the dashed curves refer to Mn in Au and the solid ones to Fe in Au.

where $\Delta\rho_0 \approx \rho_{11}(B=0)$. When $\rho_{21}(B)$ does not saturate in the fields available, $\Delta\rho_{21}$ read off a plot like Fig. 1 enables one to estimate the lower limit of $\Delta\sigma_{21}$ as $|\Delta\rho_{21}/\rho_{11}^2|$. Table I compares this quantity with the $\Delta\sigma_{21}$ obtained by direct extrapolation, as in Fig. 1.

III. DISCUSSION AND CONCLUSIONS

*Au*Fe alloys above ~11 at.% Fe contain a side-jump contribution when the temperature is increased sufficiently.[4] Equivalent plots of $\Delta\rho_{21}/\Delta\rho_0$ vs $\Delta\rho_0$, or $\Delta\rho_{21}/(\Delta\rho_0)^3$ vs $\Delta\rho_0$, show the quadratic dependence[4] of the side-jump component in the *Au*Fe alloys above ~11 at.%. We find no corresponding component for the *Au*Mn alloys of Table I. Over our measurement range ~4–250 K their $\sigma_{21}(B)$ behavior is typical of that when only skew scattering contributes to the EHE.[4] (As in *Au*Fe, the skew contribution to $\sigma_{21}^{s.o.}$ has the same sign as σ_{21}^L.) The nearest-neighbor Mn-Mn interaction is antiferromagnetic, as opposed to the ferromagnetic Fe-Fe one. The ferromagnetic environment within magnetically-coupled clusters in our *Au*Mn alloys, in which the clusters are atomically disordered regions,[8] will be

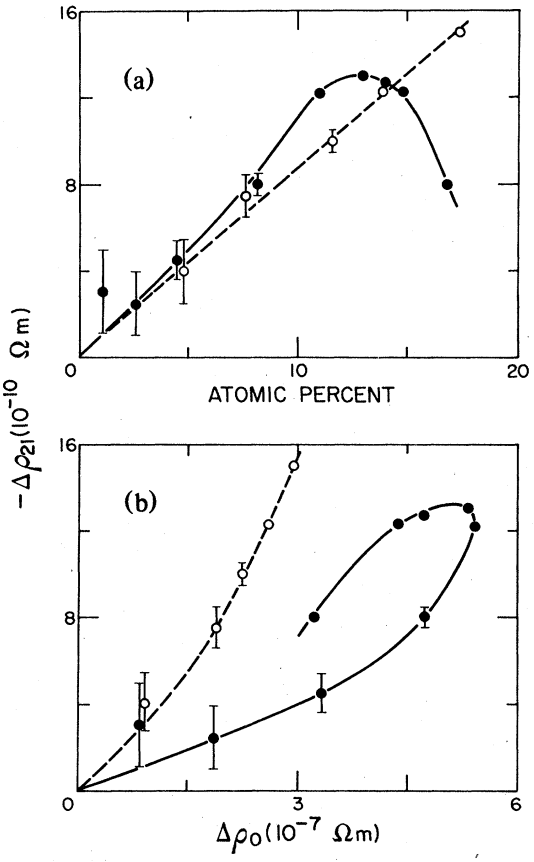

FIG. 3. As in Fig. 2, except here $\Delta\rho_{21}$ is the spin-orbit component of the Hall resistivity defined in Fig. 1.

less pronounced than in a comparable *Au*Fe alloy. Finding no evidence of side jump in *Au*Mn thus suggests that the ferromagnetic environment within the clusters of *Au*Fe is indeed crucial.

Figures 2 and 3, which plot the results of Table I in different ways, show how confusing the appearance of the spin-orbit effect can be at a given temperature (~5 K) in a system like *Au*Fe where the residual resistivity does not vary monotonically with solute concentration.[10] The ordinate in Fig. 2 is the lower limit of the spin-orbit part of the Hall conductivity, while Fig. 3 corresponds to the spin-orbit part of the Hall resistivity.

Consider first the results for *Au*Mn since they have no complication from side-jump effects. The dashed curve in Fig. 2(a) corresponds to the linear dependence of $\rho_{21}^{s_i o}$ upon concentration expected for skew scattering[1,2] and seen in Fig. 3(a). (The upswing at low concentrations in Fig. 2 reflects the singularity at zero concentration.) The dashed curve in Fig. 3(b) shows the dependence of $\Delta\rho_{21}$ upon the total amount of scattering in the alloy. Its nonlinearity follows that of the impurity resistivity. In disordered *Au*Mn alloys $\Delta\rho_0$ varies approximately linearly with concentration up to ~8 at.% but falls appreciably below the linear extrapolation as concentration is increased.[11] This drop presumably reflects the influence of the magnetically-coupled moments that form clusters at higher concentrations.[4,10,11]

In the *Au*Fe system the downturn of the solid curve in Fig. 3(a) above ~10 at.% is due to the decrease of $\Delta\rho_0$ with increasing concentration. The side-jump contribution decreases with increasing mean free path. It has the opposite sign to that of skew scattering,[4] as can be seen directly from the $\rho_{21}(B)$ curves (Fig. 1 of Ref. 4 or Fig. 2 of Ref. 14) or indirectly[14] from $\rho_{21}(T)$. The side-jump effect can be seen as the upswing of the solid curve in Fig. 2(a) above ~10 at.%. In Fig. 2(b) the curve turns back on itself because of the nonlinear variation of $\Delta\rho_0$ with concentration, and the same variation makes the behavior of $\Delta\rho_{21}$ plotted against $\Delta\rho_0$ [Fig. 3(b)] even more convoluted.

Figures 2 and 3 illustrate the difficulties of extracting the different components of the EHE in mictomagnetic alloys. It is important to note that uncovering the quadratic variation of $\sigma_{21}^{s_i o}$ upon $\Delta\rho_0$, which gives the most telling evidence for the existence of the side-jump component,[4] depends upon the consideration of $\Delta\sigma_{21}$ rather than $\Delta\rho_{21}$; a plot of $\Delta\rho_{21}/\Delta\rho_0$ vs $\Delta\rho_0$, for example, does not show the clear quadratic behavior. Another pitfall has been shown in Fig. 3 where complications from the nonlinear dependence of $\Delta\rho_0$ upon concentration could mislead the interpretation of contributing components to the EHE.

ACKNOWLEDGMENTS

We thank G. F. Turner for technical help, T. H. Saxton for measurements made during his summer studentship, and the Analysis Section of NRCC for their work done on our behalf.

[1] J. Kondo, Prog. Theor. Phys. 25, 722 (1962); A. Fert, J. Phys. Lett. (Paris) 35, L107 (1974), and references therein.

[2] A. Fert and A. Friederich, Phys. Rev. B 13, 397 (1976).

[3] J. Smit. Physica (Utrecht) 24, 39 (1958); L. Berger, Phys. Rev. B 2, 4559 (1970); P. Nozières and C. Lewiner, J. Phys. (Paris) 34, 901 (1973).

[4] C. M. Hurd and S. P. McAlister, Phys. Rev. Lett. 41, 1513 (1978).

[5] P. A. Beck, J. Less-Common Metals 28, 193 (1972).

[6] P. A. Beck, in *Magnetism in Alloys,* edited by P. A. Beck and J. T. Waber (Met. Soc. AIME, New York, 1972), p. 211.

[7] S. P. McAlister and C. M. Hurd, Phys. Rev. Lett. 37, 1017 (1976); C. M. Hurd and S. P. McAlister, Phys. Rev. B 15, 514 (1977).

[8] There is evidence (Refs. 6 and 9) that in concentrated *Au*Mn alloys the stable condition for magnetically-coupled clusters is atomically ordered. The clusters become increasingly ferromagnetic on ordering because the arrangement excludes the antiferromagnetic Mn-Mn nearest-neighbor interactions. Long-term annealing at relatively low temperatures (~600 K) promotes ordering, so we treat our samples to ensure minimum ordering in their clusters.

[9] D. J. Chakrabarti and P. A. Beck, Int. J. Magn. 3, 319 (1972).

[10] J. A. Mydosh, P. J. Ford, M. P. Kawatra, T. E. Whall, Phys. Rev. B 10, 2845 (1974).

[11] P. J. Ford and J. A. Mydosh, Phys. Rev. B 14, 2057 (1976).

[12] S. P. McAlister, L. R. Lupton, and C. M. Hurd, Solid State Commun. 25, 903 (1978).

[13] A. Friederich, A. Fert, and J. Sierro, Solid State Commun. 13, 997 (1973); J. W. F. Dorleijn and A. R. Miedema, Phys. Lett. A 55, 118 (1975); R. Huguenin and D. Rivier, Helv. Phys. Acta 38, 900 (1965).

[14] C. M. Hurd and S. P. McAlister, J. Appl. Phys. 50, 1743 (1979).